Supplementary Material: Mass measurement of graphene using quartz crystal microbalances

Robin J. Dolleman,[1,2] Mick Hsu,[1] Sten Vollebregt,[3] John E. Sader,[4] Herre S. J. van der Zant,[1] Peter G. Steeneken,[1,5] and Murali K. Ghatkesar[5]

[1)] *Kavli Institute of Nanoscience, Delft University of Technology, Lorentzweg 1, 2628 CJ, Delft, The Netherlands*

[2)] *Current affiliation: 2nd Institute of Physics, RWTH Aachen University, 52047 Aachen, Germany*[a)]

[3)] *Department of Microelectronics, Delft University of Technology, Feldmannweg 17, 2628CT, Delft, The Netherlands*

[4)] *ARC Centre of Excellence in Exciton Science, School of Mathematics and Statistics, The University of Melbourne, Victoria 3010, Australia*

[5)] *Department of Precision and Microsystems Engineering, Delft University of Technology, Mekelweg 2, 2628 CD, Delft, The Netherlands*

S1: COMMERCIALLY AVAILABLE OSCILLATOR CIRCUIT

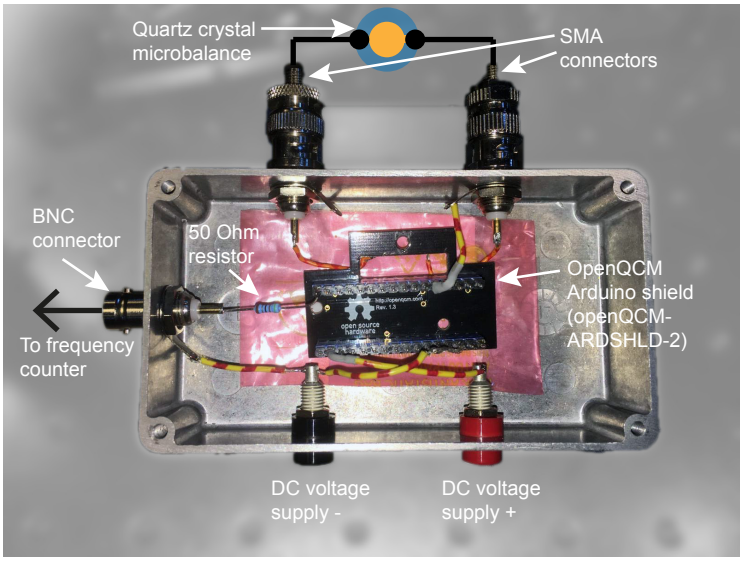

FIG. S1. Photograph of the metal boxes containing the openQCM oscillator circuit.

Part of the measurements in this work are performed by using a commercially available oscillator circuit mounted in a metal box as shown in Fig. S1. This is the openQCM Arduino shield (openQCM-ARDSHLD-2), where the crystal is normally mounted directly to the QCM using a holder. However, our application of the crystal in vacuum requires the PCB to be mounted outside the chamber. Therefore, the PCB is placed in a metal box and the connections, that normally connect directly to the crystal, are now connected to the center pins of two SMA connectors. SMA cables can then be connected to the KF-40 vacuum flange, which also uses SMA connections for the electrical feedthroughs. The DC voltage, that is normally supplied by an Arduino, is now supplied by an external voltage source (Rigol DP832A). A BNC connector carries the signal from the PCB to the frequency counter (Keysight 53230A) through a 50 Ohm resistor. This resistor matches to the load of the frequency counter and it is found that this drastically improves signal quality.

[a)] Electronic mail: dolleman@physik.rwth-aachen.de

S2: DETERMINATION OF UNCERTAINTY IN THE FREQUENCY SHIFT

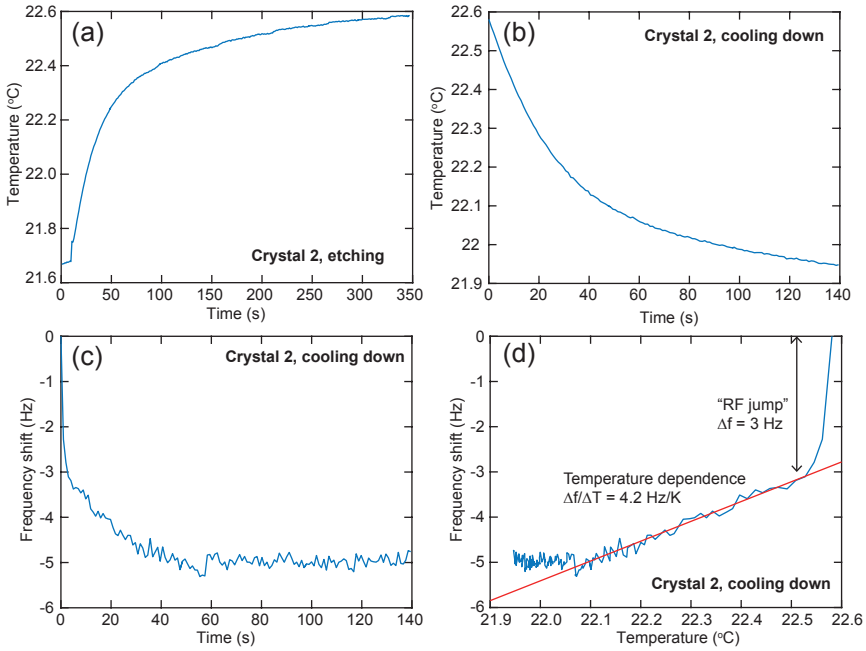

FIG. S2. Determination of the uncertainty of the frequency shift for crystal 2. (a) Temperature as function of time during the etching, the corresponding frequency shift is shown in Fig. 2(a) in the main text. (b) Temperature as function of time after etching, the RF power is switched off at $t = 0$ s. (c) Frequency shift as function of time after etching. (d) Frequency as function of temperature during cooling down, this graph is used to determine the temperature sensitivity of the crystal.

The quartz crystal microbalance is a highly sensitive platform for mass measurement, but is also sensitive to temperature and other effects which leads to some uncertainty in the measurements. For this reason, the temperature in the chamber is monitored during the etching as shown in Fig. S2(a). To give an estimate of the uncertainty, after each etching procedure the measurement of the frequency and temperature continued after the RF power was switched off. During this measurement the temperature drops (Fig. S2(b)) and a frequency shift is observed (Fig. S2(c)). Also, immediately after switching on the RF power a $\sim$3 Hz jump in the frequency is observed. The cause of this is not known, therefore we add this to the uncertainty as well. By plotting the frequency shift versus the temperature in Fig. S2(d), we determine the sensitivity of the resonance frequency to the temperature. In this crystal, the total temperature change during etching is 0.95K, resulting in a total temperature uncertainty of 4 Hz. The total uncertainty including the RF jump is then determined to be 7 Hz. In all crystals we found similar values.

For the double layer crystals the uncertainty is higher due to the occurrence of spontaneous jumps in the frequency. Most likely these can be attributed to spurious modes in the crystal or coupling to other modes. However, we cannot rule out that these jumps occur due to particles attaching or detaching to the crystal, therefore the height of these jumps was included in the uncertainty.

S3: ADDITIONAL MEASUREMENTS

Figure S3 shows additional measurements that are included in Table 1 in the main section of the paper. These measurements are taken by the oscillator circuit, but we find that the oscillator circuit becomes often becomes unstable once the RF power is switched on, and the circuit has to be reset numerous times until it locks to the correct frequency. This leads to missing data points, however the start and end frequency still provide information of the amount of mass removed from the crystal. The problem is amended by using the vector network analyzer, alternatively one could use better holders to reject the interference from the electric field inside the plasma chamber.

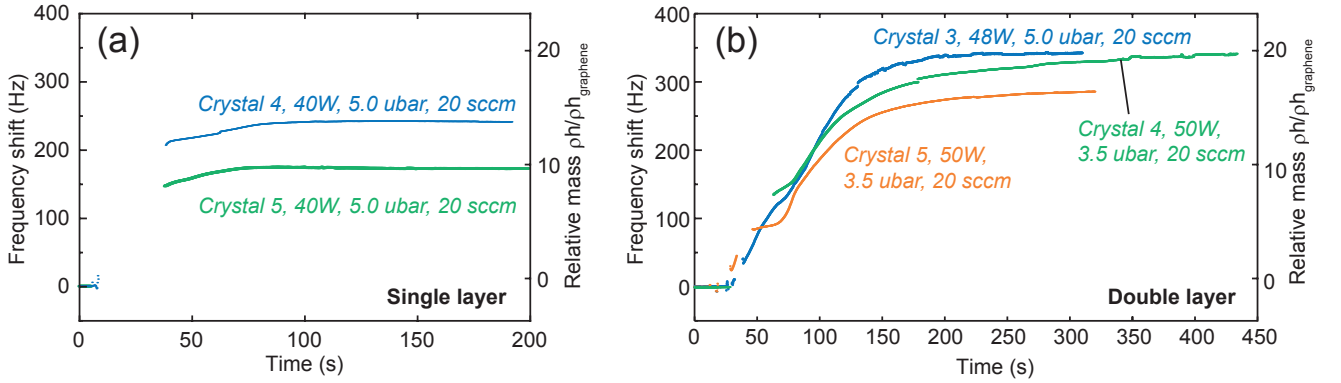

FIG. S3. Additional frequencies as function of time measured by the oscillator circuit. Note that most curves are missing data due to the oscillator circuit becoming unstable once the RF power is switched on, only the start and end frequencies are used to determine the etched mass in Table 1 in the main section of the paper. (a) Two measurements on crystals with single layer graphene. (b) Three crystals with double-layer graphene.

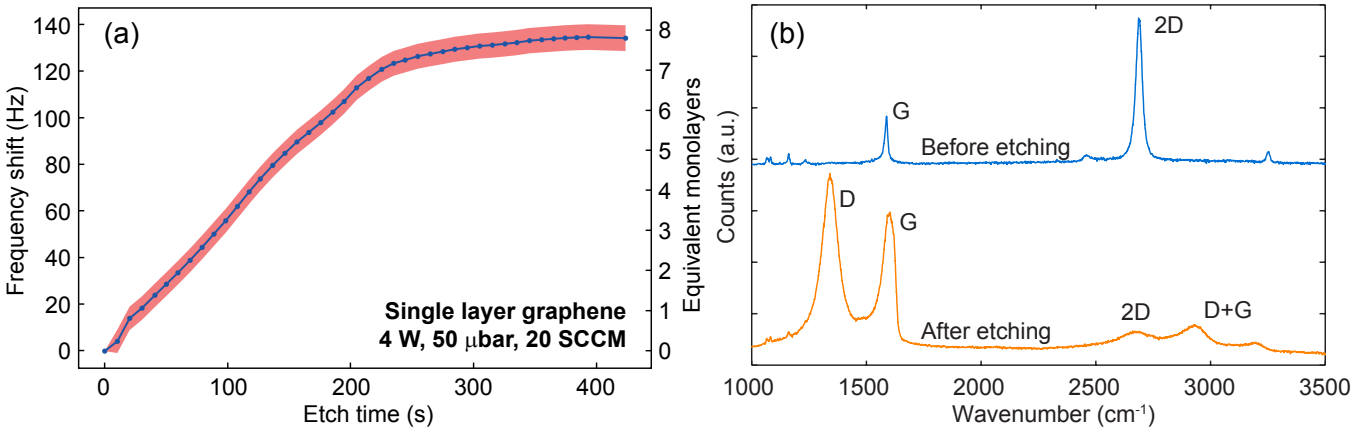

FIG. S4. Measurements at low etching power. (a) Etching curve of a single-layer graphene sample at low RF powers. (b) Raman spectrum before and after etching with low plasma power.

Measurements at low power

Figure S4(a) shows measurements at low RF powers of 4 W. We observe that the frequency increases and stabilizes at around 400 seconds. However, when Raman characterization is performed (see Fig. S4(b)), is it found that the graphene is not fully removed, and the Raman spectrum bears signatures of graphene oxide[1]. This shows that the graphene first oxidizes before it is removed from the system. In subsequent measurements a higher power was used to ensure graphene is fully removed from the crystal.

Measurements on bare crystals

Figure S5 shows measurements on a crystal without graphene that has undergone the same cleaning procedure. The RF power was switched on and off to test whether the plasma could ignite in a stable manner with this recipe and to test the stability of the frequency measurement. The frequency changes considerably during the measurement, however this can be attributed to the temperature changes in the plasma chamber. Using the frequency as function of temperature when the plasma is off, the measurement can be corrected for the temperature (red line in Fig. S5(a)). In that case, the frequency shift is less than 0.2 Hz, which is neglectable compared to the other uncertainties in the system.

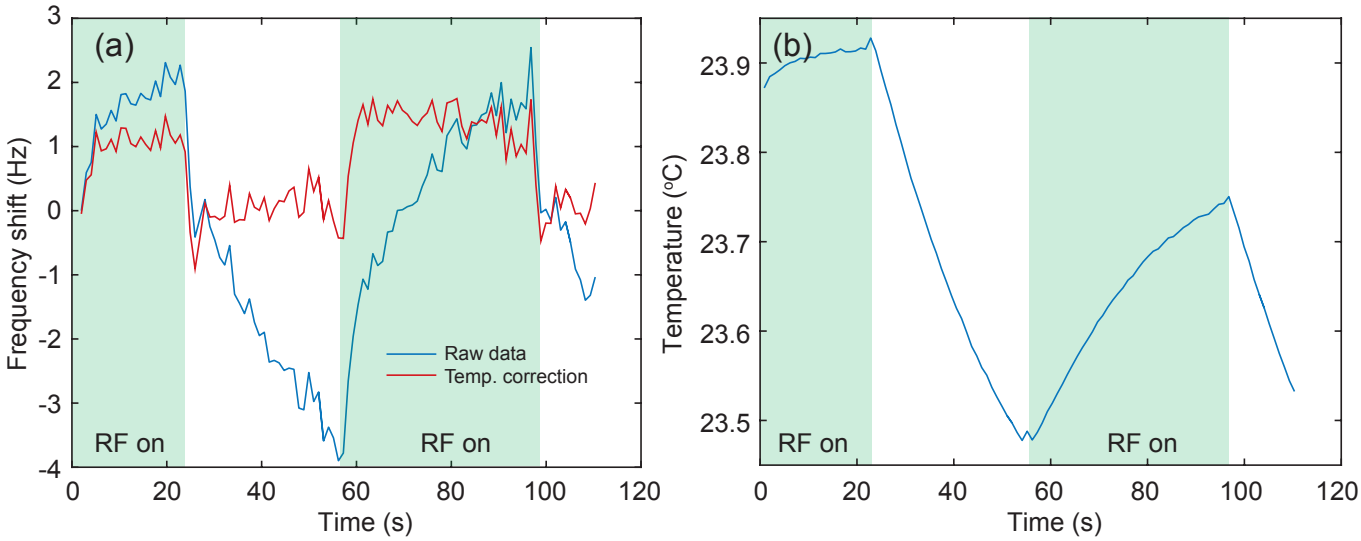

FIG. S5. Measurements on a crystal without graphene, using 20W, 50 μbar, 20 sccm oxygem plasma. (a) Frequency as function of time, the plasma was switched on and off. The temperature depencence was corrected for using the temperature-dependent frequency when the plasma was off. (b) Temperature as function of time.

Comparison of crystals covered by only polymer (without graphene) and polymer contaminated graphene layer(s)

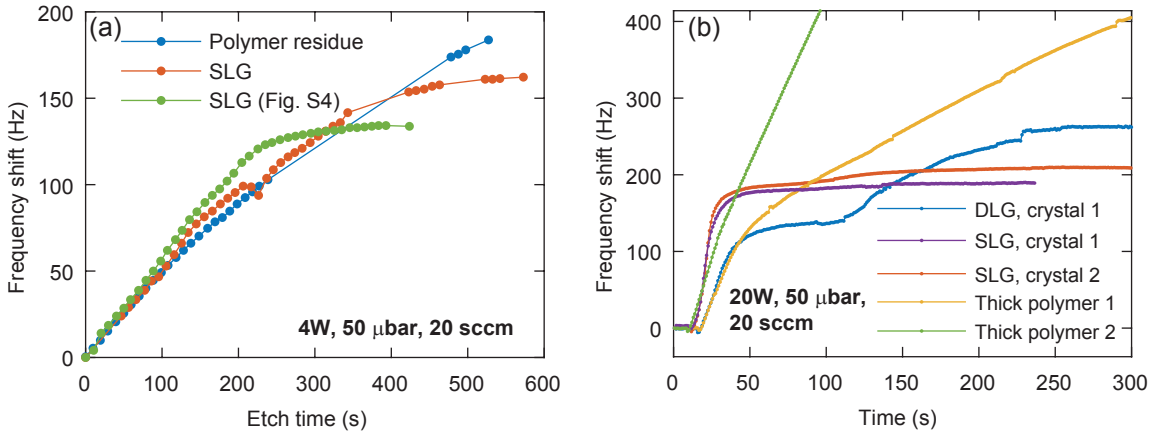

FIG. S6. (a) Measurements at low power, showing two crystals covered with single layer graphene and a crystal that has been in contact with the polymer used to transfer the graphene. These measurements are taken using the oscillator circuit. (b) Measurement at high power comparing crystals covered with graphene and crystals where the transfer polymer did not detach from the surface during transfer. These measurement are taken using the vector network analyzer (VNA).

Figure S6(a) shows measurements of the frequency shift of two crystals with single layer graphene (SLG) and a crystal on which a "dummy transfer" is performed. For "dummy transfer" the crystal was in contact with the transfer polymer, but no graphene is transfered. Comparing the slopes of the graphene-covered crystals and the crystal with polymer residue, their etching rates are similar, suggesting that our interpretation of polymer contamination is correct. At the low powers of 4W, the graphene is not fully removed (see Fig. S4) and therefore these samples are not included in the main section of the article.

Figure S6(b) compares the frequency shift of the crystals measured by the VNA in the main section of the article, to two crystals where the transfer polymer does not detach from the crystal. Therefore, much thicker polymer is left on these samples compared to Fig. S6(a). The double layer graphene (DLG) crystal shows excellent agreement in the etching rate to one of the polymer covered crystals (labeled "Thick polymer 1"). Furthermore, the etching rate of this polymer covered crystal initially increases after the plasma ignites, but then stabilizes to a slower etch rate. This could explain why the first fast etching regime in the DLG samples shows a higher rate than the second fast etching

regime. Comparing the single layer samples (SLG) to a polymer covered crystal, the graphene covered samples show a somewhat higher etching rate. This could be because the polymer residue on top of the graphene is rougher than the thick polymer that is covering the crystals, the additional surface area then allows for a faster etching rate of the polymer. Also, the close proximity of the polymer to the graphene or the gold could perhaps play a role, if these substrate materials act as a catalyst that increases the etching rate.

[1] J.-B. Wu, M.-L. Lin, X. Cong, H.-N. Liu, and P.-H. Tan, "Raman spectroscopy of graphene-based materials and its applications in related devices," Chem. Soc. Rev. **47**, 1822–1873 (2018).